Determination of the Redox Properties of Human NADPH-Cytochrome P450 Reductase†

Andrew W. Munro,*,‡ Michael A. Noble,§ Laura Robledo,§ Simon N. Daff,§ and Stephen K. Chapman§

Department of Pure & Applied Chemistry, University of Strathclyde, The Royal College, 204 George Street, Glasgow, G1 1XL, U.K., and Department of Chemistry, University of Edinburgh, The King's Buildings, West Mains Road, Edinburgh EH9 3JJ, U.K.

Received July 25, 2000; Revised Manuscript Received November 2, 2000

ABSTRACT: Midpoint reduction potentials for the flavin cofactors in human NADPH-cytochrome P450 oxidoreductase were determined by anaerobic redox titration of the diflavin (FAD and FMN) enzyme and by separate titrations of its isolated FAD/NADPH and FMN domains. Flavin reduction potentials are similar in the isolated domains (FAD domain E_1 [oxidized/semiquinone] = −286 ± 6 mV, E_2 [semiquinone/reduced] = −371 ± 7 mV; FMN domain E_1 = −43 ± 7 mV, E_2 = −280 ± 8 mV) and the soluble diflavin reductase (E_1 [FMN] = −66 ± 8 mV, E_2 [FMN] = −269 ± 10 mV; E_1 [FAD] = −283 ± 5 mV, E_2 [FAD] = −382 ± 8 mV). The lack of perturbation of the individual flavin potentials in the FAD and FMN domains indicates that the flavins are located in discrete environments and that these environments are not significantly disrupted by genetic dissection of the domains. Each flavin titrates through a blue semiquinone state, with the FMN semiquinone being most intense due to larger separation (∼200 mV) of its two couples. Both the FMN domain and the soluble reductase are purified in partially reduced, colored form from the *Escherichia coli* expression system, either as a green reductase or a gray-blue FMN domain. In both cases, large amounts of the higher potential FMN are in the semiquinone form. The redox properties of human cytochrome P450 reductase (CPR) are similar to those reported for rabbit CPR and the reductase domain of neuronal nitric oxide synthase. However, they differ markedly from those of yeast and bacterial CPRs, pointing to an important evolutionary difference in electronic regulation of these enzymes.

The cytochromes P450 (P450s)[1] are heme-containing monooxygenases critical to animal physiology and drug metabolism (*1*). Mammals possess numerous isoforms, catalyzing the oxidative metabolism of endogenous compounds such as steroids and eicosanoids, as well as a diverse array of xenobiotics (*2*, *3*). The P450s require the delivery of two electrons for catalytic function. These are delivered consecutively, the first reducing ferric substrate-bound P450 to the ferrous form. The ferrous P450 heme iron can then bind molecular oxygen (O_2). Delivery of a second electron to the ferrous-dioxygen species generates a transient ferryl-oxygen intermediate that cleaves the bound dioxygen. In the productive P450 catalytic cycle, substrate is monooxygenated and a water molecule is formed from the other oxygen atom and two protons (*4*). An efficient electron delivery system is critical to P450 catalysis, because uncoupling of electron transfer from substrate oxidation results in the diversion of reducing equivalents into the production of superoxide, hydrogen peroxide, or water. Therefore, a thorough analysis of the redox properties and enzymology of the P450's redox partner(s) is key to understanding the intricate mechanism of P450 reduction.

The cytochromes P450 can be divided conveniently into two classes, dependent on the type of reductase system. Most bacterial systems and the mitochondrial forms are class I (B-class) P450s. In these three component systems, electrons are derived from NAD(P)H and are transferred from the FAD-containing NAD(P)H ferredoxin reductase to the P450 via a small iron−sulfur-containing ferredoxin (*5*, *6*). However, the majority of eukaryotic P450s are class II (E-class), often referred to as microsomal P450s (*7*). Microsomal cytochromes P450 use a single redox partner, cytochrome P450 reductase (CPR). CPR is an FAD- and FMN-containing protein that sources its electrons from NADPH (*8*). In recent years, structures for both P450s and their redox partners from the two different classes have been solved (*9*−*15*). Arguably, the greatest successes have come with the recent solutions of a mammalian microsomal P450 and a microsomal P450 reductase (*14*, *15*).

Analysis of the amino acid sequence of microsomal CPRs indicates strong similarity to two other classes of flavoenzyme. Over approximately 200 amino acids at the N-terminal region of CPR (following the N-terminal membrane anchor region) there is strong similarity with various flavodoxins (*16*). Over the remainder of the sequence, the CPRs resemble the FAD-containing NADPH-ferredoxin (flavodoxin) reductases that are widespread in eukaryotes and prokaryotes (*17*). These similarities suggest that the CPRs have evolved as a result of a genetic fusion event and that each

† The authors thank the BBSRC, Leverhulme Trust, Royal Society and Royal Society of Edinburgh for financial support for these studies.

* To whom correspondence should be addressed. Phone/Fax: 0141 548 3727. E-mail: Andrew.Munro@strath.ac.uk.

‡ University of Strathclyde.

§ University of Edinburgh.

[1] Abbreviations: CPR, cytochrome P450 reductase; NOS, nitric oxide synthase; nNOS, neuronal nitric oxide synthase; Hq, hydroquinone; Ox, oxidized; P450, cytochrome P450 monooxygenase; Red, reduced; SHE, standard hydrogen electrode; Sq, semiquinone.

10.1021/bi001718u CCC: $20.00
Published on Web 01/20/2001

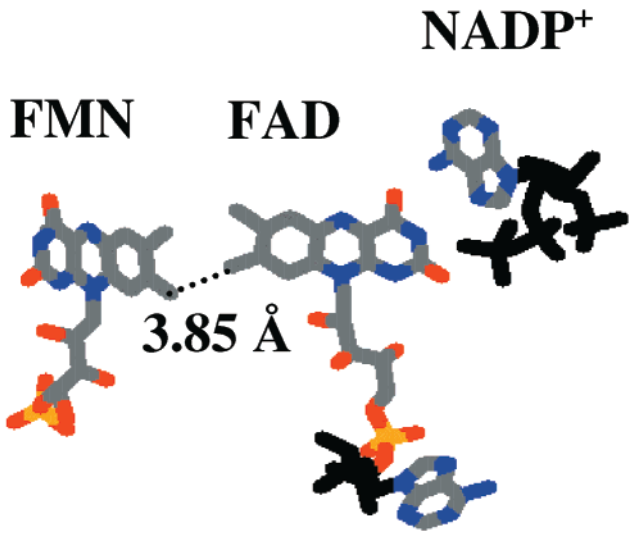

FIGURE 1: Arrangement of cofactors in NADPH-cytochrome P450 reductase. The FAD and FMN cofactors (center and right of the figure) are closely spaced in the structure of rat CPR (*15*). The closest approach between flavin methyl groups is ~3.85 Å, with no amino acid side chains between the flavin isoalloxazine ring systems. The FAD is orientated to accept reducing equivalents via hydride transfer from NADPH. $NADP^+$ (left of figure) is bound in the structure in such a position that displacement of W677 above the flavin ring system will allow the nicotinamide ring of the reduced cofactor to adopt an excellent conformation for direct hydride transfer to N_5 of the FAD. In the structure, the ribose/nicotinamide moieties of $NADP^+$ are disordered and not structurally well defined. The color scheme for the riboflavin phosphates (FAD and FMN) and adenine ring systems (FAD and $NADP^+$) of the cofactors is as follows: gray = carbon, blue = nitrogen, red = oxygen, gold = phosphorus. All other atoms are shown in black.

flavin may be contained in its own separate and distinctly folded domain (*18*). The atomic structure of the rat CPR confirms that this is the case and that the folds of the FMN and FAD/NADPH (FAD) domains of CPR resemble those of the flavodoxins and ferredoxin reductases (*19*). In rat CPR, these domains are joined by a "hinge" domain that is thought to mediate reorientation of the FAD and FMN domains with respect to one another. In the solved conformation, rat CPR domains are juxtaposed in a position favorable for direct inter-flavin electron transfer, such that the isoalloxazine dimethyl groups are located close to one another (Figure 1). In this orientation, there is an efficient pathway for electron transfer from NADPH to the FAD (by hydride transfer) and on to the FMN, without requirement for mediation via intervening amino acid side chains (*15*). The domain construction of mammalian CPR is also confirmed by the fact that the functional FAD/NADPH (amino acids 242−667) and FMN (amino acids 61−274) domains of human CPR have been successfully overexpressed and purified, and that they retain catalytic activity (*18*). The structure of the FMN domain has also been solved by NMR and has been shown to resemble strongly the flavodoxins in tertiary structure (*20*).

Knowledge of the reduction potentials of the protein-bound flavin cofactors is necessary to allow clearer understanding of the mechanism of inter-flavin and flavin−heme electron transfer processes within P450 reductase/P450 systems. In this paper, we report the first determination of the redox properties of the human cytochrome P450 reductase enzyme. The deconvolution of the redox properties of this membrane-bound diflavin enzyme is simplified by the use of a N-terminal truncated human CPR that is fully soluble in the absence of detergent and by the availability of the component FAD and FMN domains of this enzyme. This study shows that neutral blue semiquinones are stabilized on both the flavins and that the redox behavior of the flavins in the isolated domains is near identical to that in the diflavin CPR. The redox properties of human CPR are similar to those estimated previously from studies of membrane-bound rat and rabbit CPRs (*21*, *22*). With respect to the stabilization of neutral blue semiquinones on both flavins, the redox behavior of human CPR is also reminiscent of that of neuronal NOS, potentials for which we have also reported recently (*23*). However, the redox behavior of the human CPR flavins is markedly different from those of the yeast CPR and from that of well-characterized bacterial class II system (P450 BM3 from *Bacillus megaterium*), pointing to an evolutionary schism in the regulation of the redox properties of P450 reductases (*24*, *25*).

EXPERIMENTAL PROCEDURES

Overexpression and Purification of Human CPR and Its FAD and FMN Domains. Intact, soluble human cytochrome P450 reductase and its component FAD and FMN domains were expressed from T7 polymerase promoter constructs. Expression plasmid pET15b harboring the genes plus an N-terminal-located His_6 linker/thrombin cleavage site (*18*) were used to transform *Escherichia coli* strain BL21 (DE3). Culture growth and protein purification were as previously described (*18*).

Proteins were concentrated by ultrafiltration (Centricon and Centriprep tubes [Amicon]; M_r cutoffs 30 kDa for CPR and FAD domain, 10 kDa for FMN domains) to final concentrations of approximately 1 mM. Proteins were dialyzed into a solution of 50 mM Tris·HCl (pH 7.25), 1 mM EDTA containing 50% (v/v) glycerol and stored at −20 °C for less than 1 month prior to use in redox titrations.

Potentiometric Titrations. Redox titrations were performed within a Belle technology glovebox under a nitrogen atmosphere (oxygen maintained at <5 ppm) in 100 mM potassium phosphate buffer (pH 7.0) containing 10% v/v glycerol (titration buffer), at 25 ± 2 °C. Anaerobic titration buffer was prepared by flushing freshly prepared buffer with oxygen-free nitrogen. Protein samples (1−2 mL; typically, 75 μM to 1 mM) admitted to the glovebox were deoxygenated by passing through a Sephadex G25 column (1.5 × 15 cm), with final dilution of the eluted protein to 10 mL to give a typical final flavoprotein concentration of 15−100 μM. Solutions of benzyl viologen (BV), methyl viologen (MV), 2-hydroxy-1,4-naphthoquinone (HNQ), and phenazine methosulfate (PMS) were added to a final concentration of 0.5 μM as redox mediators for the titrations. Absorption spectra (350−800 nm) were recorded on a Shimadzu 2101 UV−visible spectrophotometer, and the electrochemical potential was monitored using a CD 740 pH meter (WPA) coupled to a Russell Pt/calomel electrode. The electrode was calibrated using the Fe(II)/Fe(III)-EDTA couple (108 mV) as a standard. The flavoprotein solutions were titrated electrochemically using sodium dithionite as reductant and potassium ferricyanide as oxidant, as described by Dutton (*26*). After the addition of each aliquot of reductant/oxidant

and allowing equilibration to occur (stabilization of the observed potential), 2 mL of the titrating solution was transferred to a cuvette held within the spectrophotometer. A spectrum was recorded, the potential was noted, and the solution was returned to the titration beaker. The process was repeated at several (typically, ~40) different potentials. In this way, a set of spectra representing reductive and oxidative processes was obtained. The observed potentials were those relative to the Calomel electrode, and these were corrected (using the calibration data for the Fe(II)/Fe(III)-EDTA couple) to values relative to the standard hydrogen electrode (SHE) by addition of 244 mV to the data obtained using the Pt/calomel electrode.

Treatment of Absorbance versus Potential Data. Data manipulation and analysis were performed using Origin (Microcal). For the FMN and FAD domain titrations, absorbance values at wavelengths of 474 nm (close to the absorption maximum for oxidized flavin) and 583 nm (the absorption maximum for the blue semiquinone form of flavin) were plotted against potential. For the titration data set for intact CPR, the sum of absorbance values over different wavelength ranges (450−460 nm and 580−605 nm, single wavelength intervals) were plotted against potential. Data for the titration of the individual FAD and FMN domains were fitted to eq 1, which represents a two-electron redox process derived by extension to the Nernst equation and the Beer−Lambert Law, as described previously (*25*, *26*):

$$A = \frac{a10^{(E - E_1')/59} + b + c10^{(E_2' - E)/59}}{1 + 10^{(E - E_1')/59} + 10^{(E_2' - E)/59}} \quad (1)$$

Data for the titration of the intact (diflavin) protein were fitted to eq 2, which represents the sum of two 2-electron redox processes, as described previously (*23*, *26*):

$$A = \frac{a10^{(E - E_1')/59} + b + c10^{(E_2' - E)/59}}{1 + 10^{(E - E_1')/59} + 10^{(E_2' - E)/59}} + \frac{d10^{(E - E_3')/59} + e + f10^{(E_4' - E)/59}}{1 + 10^{(E - E_3')/59} + 10^{(E_4' - E)/59}} \quad (2)$$

In these equations, A is the total absorbance, a, b, and c are component absorbance values contributed by one flavin in the oxidized, semiquinone, and reduced states, respectively, and d, e, and f are the corresponding absorbance components associated with the second flavin. E is the observed potential; E_1' and E_2' are the midpoint potentials for oxidized/semiquinone and semiquinone/reduced couples, respectively, for the first flavin, and E_3' and E_4' are the corresponding midpoint potentials for the second flavin.

In using eq 1 to fit the absorbance-potential data for the single-flavin systems (i.e., the isolated FAD and FMN domains), the variables were unconstrained, and regression analysis provided values in close agreement to those of the initial estimates. However, in utilizing eq 2 to fit the data for the diflavin system, assumptions about the values of the absorbance components were made to forbid unrealistic fitting. The complexity of the system (four-electron titration with probable overlap of midpoint potentials) necessitated employing the assumption that the oxidized flavins have equal absorbance coefficients, specifically that $a = d$. By examination of the absorption properties of the flavins in the isolated domains, we see that this is approximately true. Using this constraint, the iterative procedure yielded values of b and e that were closely similar.

RESULTS

Protein Purification. Proteins were purified to homogeneity as described previously (*18*). After harvesting the cells expressing the diflavin CPR enzyme, the cell pellet was seen to have a strong dark green color. The color became more intense after freezing of the cell pellet. This suggested that one of the two flavins existed predominantly in a blue (neutral) semiquinone form, the green color arising as a result of the mixture of blue (semiquinone flavin) and yellow (fully oxidized flavin) in the CPR enzyme. The green color was retained during purification of the CPR, and preparations of the pure enzyme reoxidized extremely slowly during storage at −20 °C, taking several weeks to convert to the fully oxidized yellow form. Visible absorbance maxima for the fully oxidized CPR were at 455 and 382 nm, with a shoulder at approximately 484 nm. When purified, the broad semiquinone band was centered at 587 nm, with a shoulder at approximately 630 nm. The fact that the stable flavin semiquinone was on the FMN was confirmed by the fact that the purified FMN domain of human CPR had a blue-grey color, as did the cells from which this domain was expressed. This finding is confirmatory of the earlier report (*18*) and supportive of other evidence indicating that it is the FMN that forms the "air stable semiquinone" in P450 reductase (*27*). Visible absorbance maxima for the fully oxidized FMN domain were at 453 and 373 nm, with a distinct shoulder on the longer wavelength band at approximately 483 nm. In the partially reduced form extracted from *E. coli*, the broad blue semiquinone band was centered at 585 nm. As with the CPR, the FMN semiquinone was stable for weeks at −20 °C. By contrast, the FAD domain of human CPR was purified in the completely oxidized (yellow) form, with visible absorbance maxima at 454 and 383 nm.

Both the pure intact CPR and FMN domains were concentrated to >1 mM prior to cryogenic storage. While the FAD domain could also be concentrated to this extent, aggregation and precipitation of a proportion of the enzyme was noted when the FAD domain was stored at high concentration for periods of several weeks at −20 °C. The FAD domain's tendency to aggregate was also observed over the several hours required to complete the reductive and oxidative titrations necessary for determination of its redox properties.

Redox Titrations. In all cases, titrations were initiated from fully oxidized protein and proceeded gradually to full flavin reduction by addition of small aliquots of sodium dithionite (from 1 and 10 mM stocks) and then again back to oxidized flavin by addition of aliquots of potassium ferricyanide stocks of the same concentration. Full equilibration was confirmed after the addition of each reducing/oxidizing aliquot by observation of a stable voltage at the electrode. No hysteretical effects were observed in any of the redox titrations. Spectra recorded at similar potentials during oxidative and reductive titrations for each of the flavoproteins were essentially identical.

Table 1: Reduction Potentials for the Flavin Cofactors in Human Cytochrome P450 Reductase[a]

	reduction potential (mV) vs standard hydrogen electrode					
	FMN cofactor			FAD cofactor		
protein	Ox/Sq	Sq/Red	Ox/Red	Ox/Sq	Sq/Red	Ox/Red
FMN domain	-43 ± 7	-280 ± 8	-162 ± 8			
FAD domain				-286 ± 6	-371 ± 7	-329 ± 7
intact CPR	-66 ± 8	-269 ± 10	-168 ± 9	-283 ± 5	-382 ± 8	-333 ± 7

[a] Potentials for the intact diflavin CPR and for the individual FAD and FMN domains were determined as described in Experimental Procedures.

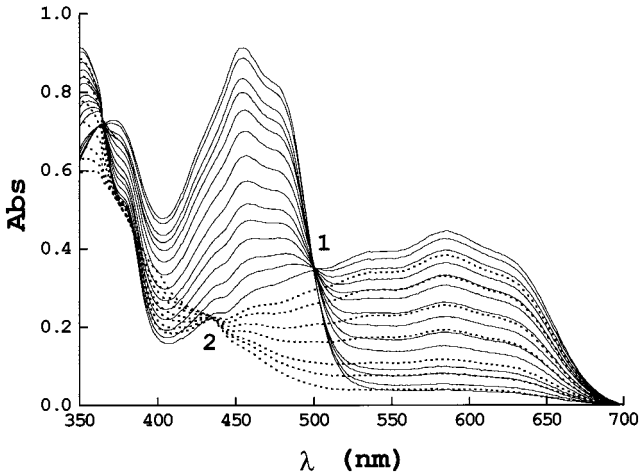

FIGURE 2: Spectral properties of human CPR FMN domain during redox titration. Spectra were recorded at several points during the redox titration of the CPR FMN domain (80 μM). The solid lines indicate spectra recorded during the addition of the first electron (oxidized to semiquinone transition), with an isosbestic point at 499 nm (indicated by "1"). The dotted lines indicate spectra recorded during addition of the second electron (semiquinone to hydroquinone transition) with an isosbestic point at 435 nm (indicated by "2"). Spectral behavior of the domain was completely reversible during oxidative and reductive titrations.

CPR FMN Domain Titration. Representative spectra of a redox titration of the isolated FMN domain are shown in Figure 2. The protein remained completely soluble and stable for the duration of the titration experiment enabling collection of good quality sets of spectra. The spectrum of fully oxidized FMN domain has a broad band maximal at 453 nm. As reduction proceeds from oxidized to the semiquinone form, the intensity of the band centered at 585 nm increases, while the band centered at 453 nm decreases. During the addition of the second electron equivalent, both the blue semiquinone signal and the 453 nm absorbance decrease in intensity. Clear isosbestic points are observed for the oxidized/semiquinone transition at 499 nm and for the semiquinone/hydroquinone transition at 435 nm. The dependences of absorbance at 475 nm and at 585 nm with potential are shown in Figure 3, panels a and b, respectively. The data for each plot are fitted to the two-electron equation (eq 1) as described in Experimental Procedures. The values of the two midpoint potentials obtained from plots a and b are in close agreement. Results are reported in Table 1. It is the large separation ($\Delta E \sim 240$ mV) between the oxidized/semiquinone and semiquinone/reduced redox couples that results in the high intensity of the blue semiquinone state. In Figure 3, panel a, it is apparent from the relative magnitudes of the two sigmoid waves that the change in absorbance coefficient at 475 nm for the oxidized/semiquinone couple is ~2-fold larger than that for the semiquinone/reduced couple. At wavelengths lower than 475 nm, the absorbance changes associated with reduction/oxidation across the semiquinone/reduced couple decrease further to reach zero absorbance change at the isosbestic point (435 nm).

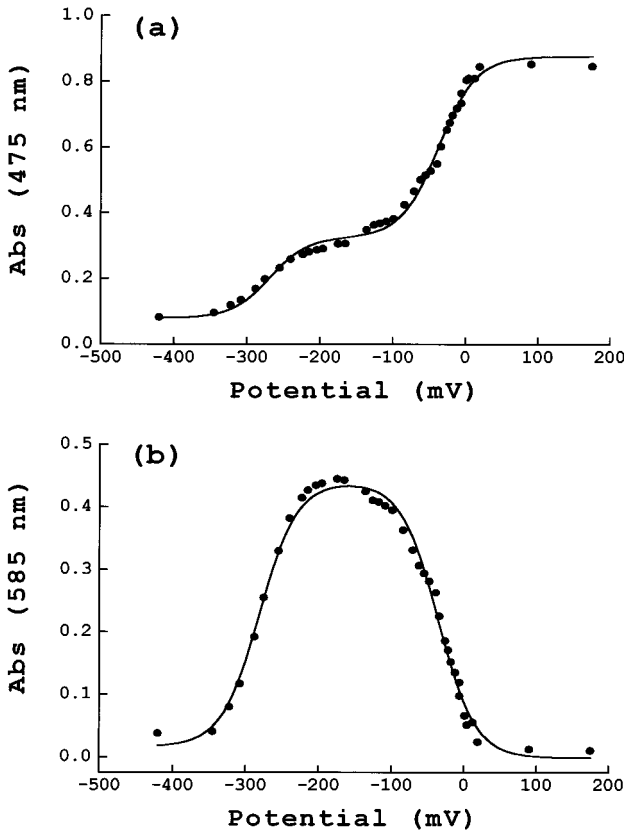

FIGURE 3: Absorbance vs potential plots for human CPR FMN domain. Panel a shows the plot of absorbance at 475 nm against reduction potential for human CPR FMN domain. At 475 nm, there is the largest overall change in flavin absorbance between fully oxidized and fully reduced forms. This wavelength is approximately intermediate between the two isosbestic points at 435 nm (semiquinone/hydroquinone) and 499 nm (oxidized/semiquinone). Panel b shows the plot of absorbance at 585 nm against reduction potential. At this wavelength, the semiquinone absorbance is near maximal and the plot follows the formation and decay of the blue FMN semiquinone species. Fits to both data sets were made using the two electron Nernst function given in Experimental Procedures (eq 1). Results are given in Table 1.

CPR FAD Domain Titration. The redox titration of the CPR FAD domain was problematical due to the tendency of the protein sample to aggregate over the period of hours at room temperature required to complete a full redox titration. This problem was also observed with the FAD domain of flavocytochrome P450 BM3 (*25*). The problem was solved by using separate FAD samples (diluted from the same stock solution of enzyme) to collect data sets (10−

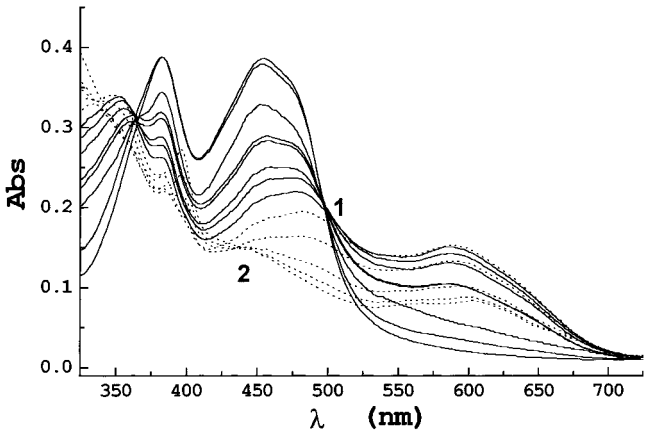

FIGURE 4: Spectral properties of human CPR FAD domain during redox titration. Spectra were recorded at several points during the redox titration of the CPR FAD domain (35 μM). The solid lines indicate spectra recorded during the addition of the first electron (oxidized to semiquinone transition), with an isosbestic point at 499 nm (indicated by "1"). The dotted lines indicate spectra recorded during addition of the second electron (semiquinone to hydroquinone transition) with an isosbestic point at 435 nm (indicated by "2").

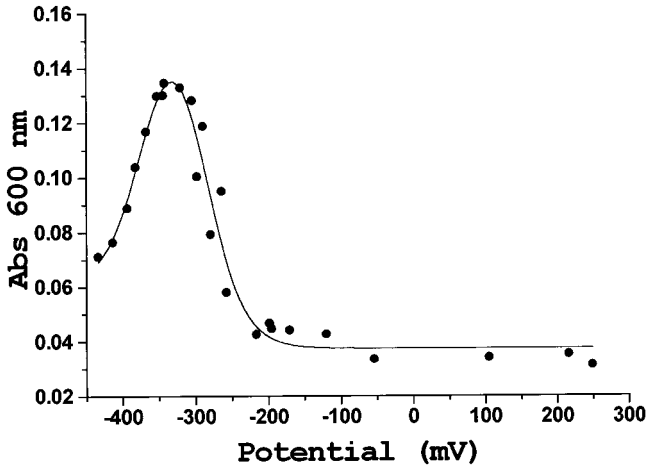

FIGURE 5: Absorbance vs potential plot for human CPR FAD domain. The plot of blue semiquinone absorbance at 600 nm against reduction potential for human CPR FAD domain. The fit to the data set was made using the two electron Nernst function given in Experimental Procedures (eq 1). Results are given in Table 1.

12 spectra) in different regions of the redox titration. Samples were exchanged when protein aggregation began to occur, as judged by increase in background absorbance (at 800 nm) to more than 0.05 units. In this way, sufficient data was obtained to determine values of the midpoint potentials of the two FAD redox couples, in the same way as was done for the FMN domain. The spectral data showed that the FAD domain also titrates through a blue semiquinone form (band maximal at ~587 nm) (Figure 4), although the semiquinone signal intensity is much lower than for the FMN domain. There are isosbestic points for the oxidized/semiquinone transition at 498 nm and for the semiquinone/hydroquinone transition at approximately 436 nm. Analysis of the data showed a much closer separation ($\Delta E \sim 85$ mV) of the two midpoint potentials as compared with the FMN domain ($\Delta E \sim 240$ mV), consistent with the weaker intensity of the blue semiquinone (Figure 5). The oxidized/semiquinone couple for the FAD domain (−283 mV) is similar to that for the semiquinone/reduced couple for the FMN domain (−269 mV), and the semiquinone/reduced couple for the FAD domain is very much more negative (−382 mV) (Table 1).

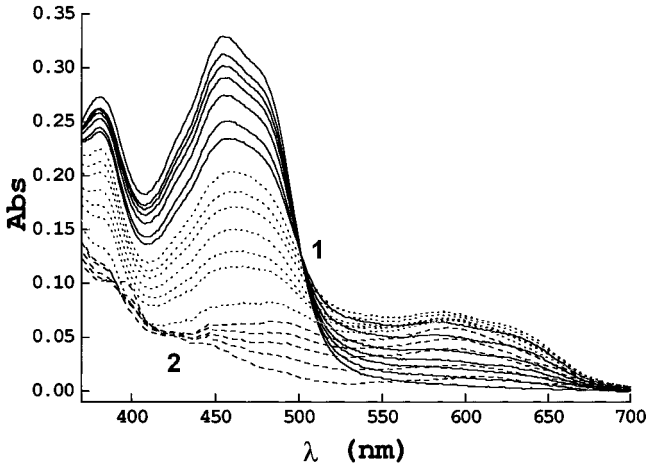

FIGURE 6: Spectral properties of intact human CPR domain during redox titration. Spectra were recorded at several points during the redox titration of intact CPR (16 μM). The solid lines indicate spectra recorded during the addition of the first electron (oxidized to semiquinone transition), with an isosbestic point at 501 nm (indicated by "1"). The dotted lines indicate spectra recorded between approximately −110 and −325 mV. The dashed lines indicate spectra at potentials more negative than −325 mV, with an isosbestic point at 429 nm (indicated by "2"). Spectral behavior of the domain was completely reversible during oxidative and reductive titrations.

Intact (FAD- and FMN-Containing) CPR Titration. Redox titations of the intact CPR did not suffer from the same turbidity problems as found with the FAD domain; thus, complete titration sets could be performed using the same enzyme batch. Clearly, the presence of the FMN-containing domain promotes solubility of the intact CPR.

Figure 6 shows a typical set of spectra obtained for a redox titration of the intact CPR protein. Three distinct phases are seen in the titration. In the first phase of the reduction process from the fully oxidized form (solid lines), there is accumulation of the semiquinone form with its broad absorbance band centered at 587 nm. In this phase of the titration (E above approximately −110 mV) an isosbestic point is evident at 501 nm. In the second phase (E from approximately −110 to −325 mV), the blue semiquinone signal remains near-maximal, while there is decreasing absorbance at lower wavelengths (dotted lines). There is no obvious isosbestic point in this phase of the titration, presumably reflecting that there are more than two species of partially reduced CPR in equilibrium in this range. These are presumably FMN semiquinone/FAD oxidized; FMN semiquinone/FAD semiquinone; and FMN hydroquinone/FAD semiquinone. In the final phase of the reduction at E more negative than −325 mV (thick solid lines), the blue semiquinone signal decreases as the FAD semiquinone is reduced to the hydroquinone. There is a second isosbestic point at approximately 429 nm in this phase of the titration.

Figure 7, panel a, shows the dependence of the summed absorbance values (single wavelength intervals) from 450 to 460 nm (across the oxidized flavin absorbance maximum) against potential. Figure 7, panel b, shows the dependence of the summed absorbances from 580 and 605 nm (across the blue semiquinone absorbance maximum). The asymmetrical bell-shape of Figure 7, panel b, clearly results from

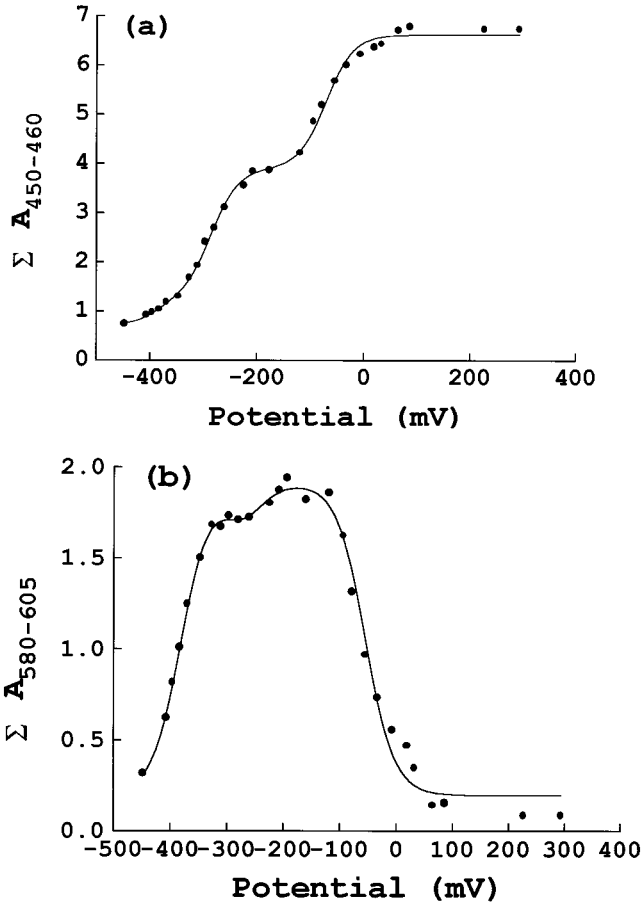

FIGURE 7: Absorbance vs potential plots for human intact CPR. Panel a shows the plot of summed absorbance values between 450 and 460 nm (across oxidized flavin maximum) against reduction potential during redox titration of intact human CPR. Panel b shows the plot of summed absorbance values between 580 and 605 nm (across semiquinone maximum) against reduction potential. Both data sets are fitted to the four-electron equation (eq 2) as described in Experimental Procedures.

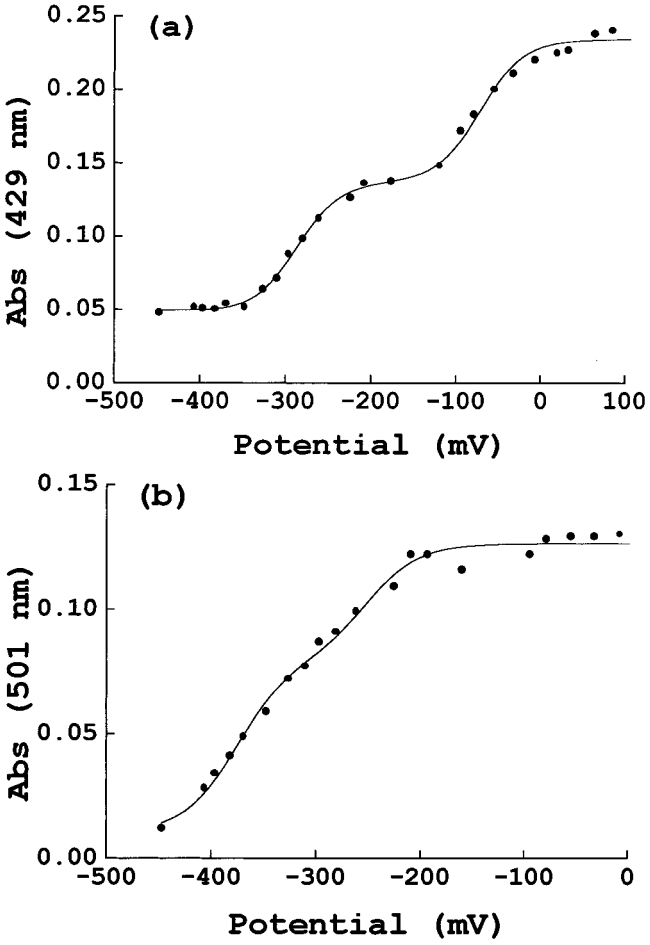

FIGURE 8: Absorbance vs potential plots for human intact CPR at isosbestic points. Panel a shows the plot of absorbance at 429 nm (approximate isosbestic point for the oxidized/semiquinone couple of both flavins) against reduction potential during redox titration of intact human CPR. Panel b shows the plot of absorbance at 501 nm (approximate isosbestic point for the semiquinone/reduced couple of both flavins) against reduction potential. Both data sets are fitted using eq 2, as described in Experimental Procedures.

two contributing semiquinone signals. The dominant (high intensity) signal is due to the FMN; the other (lower intensity) component arises from the FAD blue semiquinone. From inspection of the potential-absorbance profile shape in Figure 7, panel b, it is apparent where the approximate positions of each of the four characterizing midpoint potentials lie: the highest of the four lies on the ascending right-hand limb between 0 and −100 mV, well-separated from the other three, which lie closer together and beyond (more negative than) −200 mV. Derivation of the contributing midpoint potentials (2 × oxidized/semiquinone, 2 × semiquinone/reduced) is possible by careful analysis of both sets of data using eq 2 and making rational assumptions of the magnitudes of the contributing absorbance coefficients (see Experimental Procedures). Midpoint potentials derived from analysis of each plot must be in agreement. Hence, in Figure 7, panel a, the first of the two approximately sigmoidal "waves", located at more positive potential, is described by only one of the four potentials (oxidized/semiquinone), the second of the sigmoidal wave components (at the more negative potential) contains the remaining three midpoint potentials (the one remaining oxidized/semiquinone and two semiquinone/reduced couples). It is important to remember that the oxidized-to-semiquinone absorbance changes in this region of the spectrum are much larger in magnitude than the semiquinone-to-reduced absorbance changes.

The validity of the analysis can be tested further by plotting and analyzing absorbance-potential data at the isosbestic points for each of the two redox couples for each flavin. Each isosbestic wavelength corresponds to a near-zero absorbance change across its associated redox couple, so that an analysis of the absorbance dependence on potential yields the midpoint potential for the opposite couple. Figure 8 shows the isosbestic point absorbances plotted against potential for the data of the intact CPR redox titration. Data are fitted using the equation for the diflavin system (eq 2). In Figure 8, panel a, an analysis of the absorbance at 429 nm against potential yields the midpoint potentials for the oxidized/semiquinone couples for both FMN and FAD. In this case, variables *b* and *c* are set as constant and equal (the absorbance values for semiquinone and reduced states of one flavin, respectively, equal at the isosbestic point), as are *e* and *f* (the corresponding absorbances of semiquinone and reduced states of the second flavin, again equal at the isosbestic point) (see eq 2). Conversely, analysis of the absorbance at 501 nm versus potential (Figure 8, panel b) yields the midpoint potentials for the semiquinone/reduced

couples for both FMN and FAD. In this case, variables are fixed such that $a = b$ and $d = e$ are set constant and equal in the fitting procedure. The two midpoint potentials associated with one isosbestic point (e.g., both FMN and FAD oxidized/semiquinone) were held fixed in the first fitting procedure, at values determined from fits to the other data sets. The resultant midpoint potentials derived by this fitting for the other two couples (e.g., FMN and FAD semiquinone/reduced) were then used as the "fixed" potentials in the next round of analysis for the data of the other isosbestic point. Successive rounds of analysis were performed until there were no further changes in midpoint potentials. The values for the midpoint potentials determined by these analyses are very close to those determined by the other approaches and demonstrate that the analytical methods are soundly based. The values of the midpoint potentials for the intact CPR are recorded in Table 1 and take into account the statistical variations of the individual values determined from each of the four different fitting procedures outlined above.

DISCUSSION

The reduction potentials that we present for the human isoform of P450 reductase indicate that the redox properties of human CPR are similar to those estimated previously for the rabbit isoform by Iyanagi and co-workers (*21*), although the most positive potential (the FMN ox/sq couple) of human CPR is >40 mV more positive than that of the rabbit isoform. The electron transfer pathway (from NADPH hydride transfer to FAD to FMN to P450) is clearly established, but the actual mechanism of electron transfer through the flavins and the redox cycling of the electrons through the flavins is not. Availability of flavin midpoint potentials, together with flavin electron-transfer kinetic data (see accompanying paper in this issue by Scrutton and co-workers) has helped to address these points.

The reduction potentials of the flavins in various members of the CPR family have now been determined (Figure 9). The redox properties of the flavins in human CPR are also similar to those of the reductase domain of neuronal nitric oxide synthase (nNOS) (*23*). However, there are differences in the order of the couples between nNOS reductase and the CPRs. In nNOS reductase, the oxidized/semiquinone couple of the FAD has a more positive potential than the semiquinone/hydroquinone couple of the FMN. The reverse is the case for the intact human CPR. However, these mammalian enzymes have considerably different redox properties to those measured for a bacterial (P450 BM3) CPR and to those estimated for yeast (*S. cerevisiae*) reductase. In both these enzymes, only one of the flavins (the FAD) stabilizes a blue semiquinone. This points to a possible evolutionary schism between CPRs from bacteria and lower eukaryotes and their counterparts in higher eukaryotes. Mammalian CPRs form an air stable semiquinone (on the FMN) and are reduced to a three-electron reduced form after addition of NADPH. This oxidizes by two successive electron transfers from the FMN to the P450, returning the enzyme to its normal resting (FMN semiquinone) form. Thus, mammalian CPRs usually cycle between reduction states of 1−3−2−1 during catalysis of P450 reduction, where the numbers refer to the total number of electrons on the flavins. In contrast, the P450 BM3 reductase is actually inactivated if the 3-electron reduced (i.e. FMN hydroquinone, FAD semiquinone) form accumulates (*28*). This suggests that important enzyme regulatory phenomena underlie the distinct redox behavior of these CPRs. P450 BM3 reductase (and, possibly, *Saccharomyces cerevisiae* CPR) is fully oxidized in the resting state and undergoes a reduction cycle of 0−2−1−0 after reduction by NADPH (*29*). In the two-electron reduced form, reduction potentials suggest that the enzyme should be in the FMN hydroquinone form. However, EPR studies of the enzyme during catalysis suggest that both flavins form semiquinones (*30*). This raises the interesting question as to the influence of the bound pyridine nucleotide (NADPH/$NADP^+$) on the flavin redox properties. Previously, we have shown that the binding of a nucleotide analogue perturbs FAD potentials in *E. coli* flavodoxin reductase (*16*).

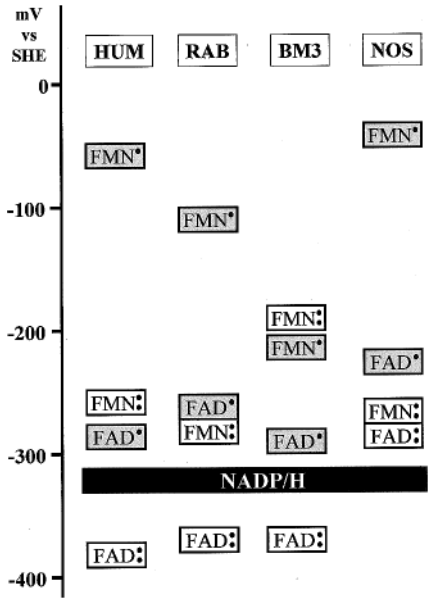

FIGURE 9: Flavin reduction potentials in the CPR enzyme family. The relative reduction potentials of the FMN oxidized/semiquinone (gray box) and semiquinone/hydroquinone (white box) are shown for different members of this diflavin enzyme family. Dots indicate electrons: one electron for semiquinone and two for hydroquinone flavin. The scheme shows the values for human (Hum), rabbit (Rab) and *Bacillus megaterium* (BM3) CPRs and for the CPR domain of rat neuronal nitric oxide synthase (NOS). The black bar indicates the reduction potential of the $NADP^+$/NADPH couple.

In recent studies (*23*), we showed that the flavin potentials of nNOS were little altered in the presence or absence of the activator molecule Ca^{2+}/calmodulin. These findings were consistent with Ca^{2+}/calmodulin-induced structural rearrangement as a means of triggering enhanced electron transfer in this enzyme, as opposed to the activator altering the driving force (i.e., changing reduction potentials) for electron transfer between the flavins and between FMN/heme in this flavocytochrome. This, in turn, is consistent with the only structural data available for a CPR enzyme. In the rat CPR structure, it is evident that the enzyme has two distinct flavin domains (the ferredoxin reductase-like FAD/NADPH domain and the flavodoxin-like FMN domain) linked by a large "hinge" domain that facilitates movement of the two flavin domains. Presumably, interaction with Ca^{2+}/calmodulin [and possibly the binding and dissociation of NADP-($^+$/H)] affects domain movement. In the rat CPR structure, the rotation of reduced FMN domain away from the FAD/NADPH domain is probably critical to expose this flavin for interaction with the P450 redox partner. One finding from

our redox titrations of intact human CPR may provide some evidence for the importance of structural changes in this enzyme. Prior to initiation of redox titrations, the pure green (single semiquinone) form of CPR was oxidized fully using ferricyanide. It was noted that oxidation of this form was unusually slow and that equilibration of the system required much longer than when the experiment was performed in reverse (i.e., addition of the first electron to oxidized CPR using dithionite). We consider that the purified semiquinone form of human CPR may be in a kinetically "trapped" form that protects the semiquinone FMN and is slow to undergo conformational changes as the FMN is completely oxidized.

In conclusion, we have determined the reduction potentials of the human form of P450 reductase and provided evidence that molecular dissection of the reductase into component mono-flavin domains does not perturb significantly the redox properties of the bound cofactors. The accompanying paper in this issue addressed intriguing questions regarding the mechanisms of this enzyme. In ongoing studies, we are also examining the possibility that the bound pyridine nucleotide perturbs the redox properties of CPR, by re-determining the potentials of the system with a redox-inactive analogue of NADPH bound to the CPR (*31*).

ACKNOWLEDGMENT

The authors thank Dr. Mark Paine and Prof. Roland Wolf for provision of clones encoding human CPR and its domains.

REFERENCES

1. Lewis, D. F. V. (1996) In *Cytochromes P450: Structure, Function and Mechanism* (Lewis, D. F. V., Ed.) pp 115−167, Taylor and Francis, London.
2. Nelson, D. R., Koymans, L., Kamataki, T., Stegeman, J. J., Feyereisen, R., Waxman, D. J., Waterman, M. R., Gotoh, O., Coon, M. J., Estabrook, R. W., Gunsalus, I. C., and Nebert, D. W. (1996) *Pharmacogenetics 6*, 1−42.
3. Porter, T. D., and Coon, M. J. (1991) *J. Biol. Chem. 266*, 13469−13472.
4. Ortiz de Montellano, P. R. (1995) In *Cytochrome P450: Structure, Mechanism and Biochemistry* (Ortiz de Montellano, P. R., Ed.) 2nd ed., pp 245−303, Plenum Press, New York.
5. Munro, A. W., and Lindsay, J. G. (1996) *Mol. Microbiol. 20*, 1115−1125.
6. Sligar, S. G. (1976) *Biochemistry 15*, 5399−5406.
7. Guengerich, F. P. (1992) *FASEB J. 6*, 745−748.
8. Iyanagi, T., and Mason, H. S. (1973) *Biochemistry 12*, 2297−2308.
9. Poulos, T. L., Finzel, B. C., and Howard, A. J. (1987) *J. Mol. Biol. 195*, 687−700.
10. Ravichandran, K. G., Boddupalli, S. S., Peterson, J. A., and Deisenhofer, J. (1993) *Science 261*, 731−736.
11. Pochapsky, T. C., Jain, N. U., Kuti, M., Lyons, T. A., and Heymont, J. (1999) *Biochemistry 38*, 4681−4690.
12. Pikuleva, I. A., Tesh, K., Waterman, M. R., and Kim, Y. C. (2000) *Arch. Biochem. Biophys. 373*, 44−55.
13. Hasemann, C. A., Ravichandran, K. G., Peterson, J. A., and Deisenhofer, J. (1994) *J. Mol. Biol. 236*, 1169−1185.
14. Williams, P. A., Cosme, J., Sridhar, V., Johnson, E. F., and McRee, D. E. (2000) *Mol. Cell 5*, 121−131.
15. Wang, M., Roberts, D. L., Paschke, R., Shea, T. M., Masters, B. S. S., and Kim, J.-J. P. (1997) *Proc. Natl. Acad. Sci. U.S.A. 94*, 8411−8416.
16. McIver, L., Leadbeater, C., Campopiano, D. J., Baxter, R. L., Daff, S. N., Chapman, S. K., and Munro, A. W. (1998) *Eur. J. Biochem. 257*, 577−585.
17. Bruns, C. M., and Karplus, P. A. (1995) *J. Mol. Biol. 247*, 125−145.
18. Smith, G. C. M., Tew, D. G., and Wolf, C. R. (1994) *Proc. Natl. Acad. Sci. U.S.A. 91*, 8710−8714.
19. Jenkins, C. M., and Waterman, M. R. (1998) *Biochemistry 37*, 6106−6113.
20. Zhao, Q., Modi, S., Smith, G., Paine, M., McDonagh, P. D., Wolf, C. R., Tew, D., Lian, L. Y., Roberts, G. C. K., and Driessen, H. P. C. (1999) *Protein Science 8*, 298−306.
21. Iyanagi, T., Makino, N., and Mason, H. S. (1974) *Biochemistry 13*, 1701−1710.
22. Vermillion, J. L., and Coon, M. J. (1978) *J. Biol. Chem. 253*, 8812−8819.
23. Noble, M. A., Munro, A. W., Rivers, S. L., Robledo, L., Daff, S. N., Yellowlees, L. J., Shimizu, T., Sagami, I., Guillemette, J. G., and Chapman, S. K. (1999) *Biochemistry 38*, 16413−16418.
24. Louerat-Oriou, B., Perret, A., and Pompon, D. (1998) *Eur. J. Biochem. 258*, 1040−1049.
25. Daff, S. N., Chapman, S. K., Turner, K. L., Holt, R. A., Govindaraj, S., Poulos, T. L., and Munro, A. W. (1997) *Biochemistry 36*, 13816−13823.
26. Dutton, P. L. (1978) *Methods Enzymol. 54*, 411−435.
27. Vermillion, J. L., and Coon, M. J. (1978) *J. Biol. Chem. 253*, 2694−2704.
28. Narhi, L. O., and Fulco, A. J. (1986) *J. Biol. Chem. 261*, 7160−7169.
29. Murataliev, M. B., and Feyereisen, R. (1996) *Biochemistry 35*, 15029−15037.
30. Murataliev, M. B., Klein, M., Fulco, A., and Feyereisen, R. (1997) *Biochemistry 36*, 8401−8412.
31. Murataliev, M. B., and Feyereisen, R. (2000) *Biochemistry 39*, 5066−5074.

BI001718U